

New highly fluorescent pH indicator for ratiometric RGB imaging of pCO₂

This content has been downloaded from IOPscience. Please scroll down to see the full text.

2014 Methods Appl. Fluoresc. 2 024001

(<http://iopscience.iop.org/2050-6120/2/2/024001>)

View [the table of contents for this issue](#), or go to the [journal homepage](#) for more

Download details:

IP Address: 134.245.215.185

This content was downloaded on 17/06/2014 at 09:22

Please note that [terms and conditions apply](#).

New highly fluorescent pH indicator for ratiometric RGB imaging of pCO₂

Susanne Schutting¹, Ingo Klimant¹, Dirk de Beer² and Sergey M Borisov¹

¹ Institute of Analytical Chemistry and Food Chemistry, Graz University of Technology, Stremayrgasse 9, A-8010, Graz, Austria

² Max-Planck-Institute of Marine Microbiology, Celsiusstrasse 1, D-28359, Bremen, Germany

E-mail: sergey.borisov@tugraz.at

Received 24 October 2013, revised 8 December 2013

Accepted for publication 18 December 2013

Published 9 April 2014

Abstract

A new diketo-pyrrolo-pyrrole (DPP) indicator dye for optical sensing of carbon dioxide is prepared via a simple one step synthesis from commercially available low cost 'Pigment Orange 73'. The pigment is modified via alkylation of one of the lactam nitrogens with a *tert*-butylbenzyl group. The indicator dye is highly soluble in organic solvents and in polymers and shows pH-dependent absorption (λ_{\max} 501 and 572 nm for the protonated and deprotonated forms, respectively) and emission spectra (λ_{\max} 524 and 605 nm for the protonated and deprotonated forms, respectively). Both the protonated and the deprotonated forms show high fluorescence quantum yields (Φ_{prot} 0.86; Φ_{deprot} 0.66). Hence, colorimetric read-out and ratiometric fluorescence intensity measurements are possible. The emission of the two forms of the indicator excellently matches the response of the green and the red channels of an RGB camera. This enables imaging of carbon dioxide distribution with a simple and low cost optical set-up. The sensor based on the new DPP dye shows very high sensitivity and is particularly promising for monitoring atmospheric levels of carbon dioxide.

Keywords: optical sensor, fluorescence, absorption, carbon dioxide, imaging

 Online supplementary data available from stacks.iop.org/MAF/2/024001/mmedia

1. Introduction

Carbon dioxide is one of the most important parameters for environmental monitoring, marine research and oceanography. The increase of carbon dioxide concentration in the oceans causes acidification, which severely affects the flora and fauna therein [1–6]. The analytical tools for detection of dissolved carbon dioxide are limited to only a few such as the Severinghaus electrode [7] or IR analyzers. The former suffers from electromagnetic interferences and has slow response. IR analyzers are fast [8], but are mostly suitable for measurements in gaseous phase [9, 10] since water causes a significant interference. Several new concepts of carbon dioxide chemosensors were published in recent years [11–15]; however so called 'plastic type' sensors remain the most common ones [16, 17]. These materials contain a pH-sensitive dye and a base (most commonly a quaternary ammonium base) dissolved in a polymer matrix. The pH indicator

responds to the analyte by altering its optical properties, mostly the absorption or emission characteristics. In case of the fluorescent sensors referencing of the fluorescence intensity is required to enable reliable measurements. This can be achieved by adding a second analyte-insensitive dye which emission spectrum is clearly separated from that of the indicator (ratiometric read-out) or which luminescence decay time is significantly different from the lifetime of the indicator (dual lifetime referencing scheme) [18–20]. In both schemes photobleaching (indicator, reference dye or both) causes a dramatic change of the emission ratio of the indicator and the reference dye. Therefore, self-referencing indicator dyes are highly desirable; however only a few such dyes have been reported [21–24]. Spectral compatibility with commercially available red/green/blue (RGB) cameras is also of great interest. The read-out with RGB cameras is a simple and low cost technique for imaging different parameters such as CO₂ [25], pH [26–29] or oxygen [30–33], to name only

a few. Recently, we presented a new class of pH-sensitive indicator dyes based on diketo-pyrrolo-pyrroles (DPPs) [29, 34]. DPPs are usually insoluble in organic solvents and are mainly used as pigments [35]. The soluble derivatives (mainly *N*-alkylated dyes) [36–43] are also of much practical interest and are applied e.g. in photovoltaics [37–39]. So far only a few applications of DPPs as fluorescent probes are found in the literature [29, 44–46]. The new DPP-based pH indicators were shown to be highly promising for application in optical pH and carbon dioxide sensors [29, 34]. Particularly, dual emission from the protonated and deprotonated forms enabled ratiometric read-out, but the emission from the deprotonated form was much weaker than that of the protonated form ($\Phi_{\text{prot}} \approx 1$ and $\Phi_{\text{deprot}} \approx 0.1$). Unfortunately, these dually emitting dyes were not fully compatible with the green and red channels of the digital cameras [47]. In this study, we present a new DPP-based pH indicator which overcomes these drawbacks. It will be shown that the new dye possesses high fluorescence quantum yields for both the protonated and the deprotonated form and is excellently suitable for the RGB read-out. The CO₂ sensor shows very high sensitivity and is particularly useful for monitoring atmospheric levels of the analyte.

2. Experimental details

2.1. Materials

1,4-diketo-3,6-bis(4-*tert*-butyl-phenyl)-2,5-dihydro pyrrolo [3,4-*c*]pyrrole (Pigment Orange 73), 1,6,7,12-tetraphenoxy-*N,N'*-bis(2,6-diisopropylphenyl)-perylene-3,4,9,10-tetracarboxylic bisimide (Lumogen-red) and *N,N'*-bis(2,6-diisopropylphenyl)-perylene-3,4,9,10-tetracarboxylic bisimide (Lumogen-orange) were purchased from Kremer Pigments (Germany, www.kremer-pigmente.com). Ethyl cellulose 49 (EC49, ethoxyl content 49%), sodium sulfate (anhydrous), sodium *tert*-butoxide, 4-*tert*-butylbenzyl bromide, tetraoctylammonium hydroxide solution (TOAOH, 20% in methanol) and anhydrous dimethylformamide were obtained from Sigma-Aldrich (www.sigmaaldrich.com). All other solvents were purchased from VWR (Austria, www.vwr.com). The silicone components: vinyl terminated polydimethylsiloxane (viscosity 1000 cSt.), (25–35% methylhydro-siloxane)-dimethylsiloxane copolymer (viscosity 25–35 cSt.), 1,3,5,7-tetravinyl-1,3,5,7-tetramethylcyclotetrasiloxane and the platinum–divinyltetramethylsiloxane complex were received from ABCR (Germany, www.abcr.de). Ultrafine hydrophobic titanium dioxide P170 was purchased from Kemira (www.kemira.com). High purity nitrogen, 5% carbon dioxide in nitrogen, 0.2% carbon dioxide in nitrogen and carbon dioxide were obtained from Air Liquide (Austria, www.airliquide.at). Poly(ethylene terephthalate) (PET) support Melinex 505 was obtained from Pütz (Germany, www.puetz-folien.com). Silica gel was received from Roth (www.carlroth.com). Synthesis of BiPh-DiSA (3,6-bis[4'-bis(2-ethylhexyl)sulfonylamide-1,1'-biphenyl-4-yl]-2,5-dihydro pyrrolo[3,4-*c*]pyrrole-1,4-dione) and MoPh-DiSA (3,6-bis[4-bis(2-ethylhexyl)sulfonylamide-phenyl]-2,5-dihydro pyrrolo[3,4-*c*]pyrrole-1,4-dione) was described before [34].

2.2. Synthesis of 2-hydro-5-*tert*-butylbenzyl-3,6-bis(4-*tert*-butyl-phenyl)-pyrrolo[3,4-*c*]pyrrole-1,4-dione (DPpTBu³)

Pigment orange 73 (2 g, 4.9 mmol) and sodium *tert*-butoxide (0.96 g, 10 mmol) were dissolved in anhydrous dimethylformamide (80 ml). 4-*tert*-butylbenzyl bromide (1.1 ml, 6.0 mmol) was added dropwise. After stirring for 8 h at 60 °C the mixture was diluted with deionized water. The dye was extracted with dichloromethane and hydrochloric acid and sodium chloride were added to facilitate the phase separation. The organic phase was collected, dried over anhydrous sodium sulfate and evaporated to dryness under reduced pressure. The crude product was purified via column chromatography on silica gel using dichloromethane/tetrahydrofuran (98:2). The product was dissolved in dichloromethane and precipitated with hexane to give an orange powder (0.23 g, 8.3% of theoretical yield of DPpTBu³).

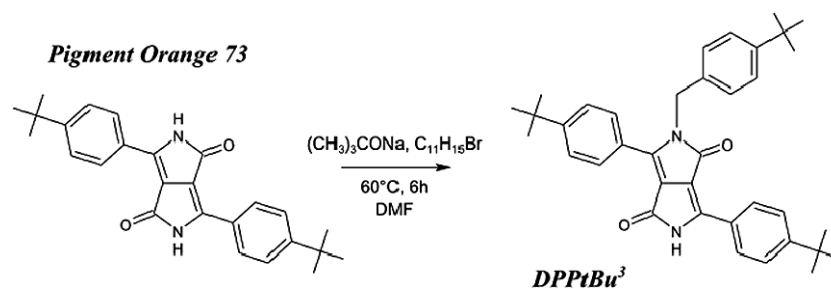
DI-EI-TOF: m/z of $[\text{MH}]^+$ found 546.3259, calculated 546.3246. ¹H NMR (300 MHz, CDCl₃) δ 9.38 (s, 1H), 8.28 (d, 2H), 7.77 (d, 2H), 7.53 (d, 2H), 7.50 (d, 2H), 7.34 (d, 2H), 7.16 (d, 2H), 5.04 (s, 2H), 1.35 (s, 18H), 1.30 (s, 9H). Analysis for C₃₇H₄₂N₂O₂ found: C81.12, H7.59, N5.12, calculated: C81.28, H7.74, N5.12.

2.3. Preparation of the planar optodes

'Cocktail 1' containing X mg of the dye and 100 μl of the tetraoctylammonium hydroxide solution (20% TOAOH in methanol) was purged with carbon dioxide gas. X was 3.0 mg and 0.5 mg for the absorption and emission measurements, respectively. 'Cocktail 2' containing 200 mg ethyl cellulose (EC49) dissolved in 3800 mg of a toluene:ethanol mixture (6:4 w/w) was added to the 'cocktail 1'. The resulting solution was knife-coated on a dust-free PET or glass support. A sensing film of $\sim 7.5 \mu\text{m}$ thickness was obtained after evaporation of the solvent. The sensing film was covered with a gas-permeable $\sim 22 \mu\text{m}$ -thick silicone layer by knife-coating 'cocktail 3' consisting of 800 mg vinyl terminated polydimethylsiloxane, 32 μl (25–35% methylhydro-siloxane)-dimethylsiloxane copolymer, 2 μl 1,3,5,7-tetravinyl-1,3,5,7-tetramethylcyclotetrasiloxane and 4 μl platinum–divinyltetramethylsiloxane complex dissolved in 1600 mg hexane. For emission measurements a similar layer was prepared but 200 mg of titanium dioxide were dispersed in 'cocktail 3'. The sensors were kept in an oven (60 °C) for 10–15 min to complete polymerization of the silicone rubber.

2.4. Methods

¹H NMR spectra were recorded on a 300 MHz instrument (Bruker) in CDCl₃ with TMS as standard. Absorption spectra were recorded on a Cary 50 UV–vis spectrophotometer (www.varianinc.com). Determination of the molar absorption coefficients was carried out as an average of three independent measurements. Photobleaching experiments were performed by irradiating the samples (2.5 ml) with the light of a high-power 10 W LED array (λ_{max} 458 nm, 3 LEDs, www.led-tech.de) operated at 6 W input power. A lens



Scheme 1. Synthesis of DPtBu³ starting from Pigment Orange 73.

(Edmund optics, www.edmundoptics.de) was used to focus the light of the LED array on the glass cuvette (photon flux: $\sim 4000 \mu\text{mol s}^{-1} \text{m}^2$ as determined with a Li-250A light meter from Li-COR, www.licor.com). The photodegradation profiles were obtained by monitoring the absorption spectra of the respective dye dissolved in tetrahydrofuran and represented an average from three independent experiments. The solutions were homogenized by shaking after each illumination period. Fluorescence spectra were recorded on a Hitachi F-7000 fluorescence spectrometer (www.hitachi.com) equipped with a red-sensitive photomultiplier R928 from Hamamatsu (www.hamamatsu.com). Relative fluorescence quantum yields were determined according to Demas and Crosby [48]. The solutions of Lumogen-orange ($\Phi \approx 1$) and Lumogen-red ($\Phi \approx 0.96$) [49, 50] in chloroform were used as standards for the protonated and the deprotonated form, respectively. Three independent measurements were performed for determination of the relative quantum yields and the average value obtained was used. In case of the sensing materials only the absolute quantum yields were determined. These measurements were performed on a Fluorolog3 fluorescence spectrometer (www.horiba.com) equipped with a NIR-sensitive photomultiplier R2658 from Hamamatsu (300–1050 nm) and an integrating sphere (Horiba).

Gas calibration mixtures were obtained using a gas mixing device from MKS (www.mksinst.com). The gas mixture was humidified to about 85% relative humidity (saturated KCl solution) prior entering the calibration chamber. Temperature was controlled by a cryostat ThermoHaake DC50. Photographic images were acquired with a Canon 5D camera equipped with a Canon 24-105L objective and two layers of a LEE plastic filter ‘spring yellow’. The same high-power 10 W LED array (λ_{max} 458 nm, 3 LEDs, www.led-tech.de) as for the photodegradation experiments combined with a short-pass BG-12 filter served as an excitation source.

3. Results and discussion

3.1. Synthesis

The DPP chromophores possess planar structure and are poorly soluble in organic solvents [51]. Low solubility prevents the dyes from application as indicators in optical sensors. We previously demonstrated that the dyes are pH-sensitive due to the deprotonation of the lactam nitrogen [29, 34]. Modification of the phenyl rings with bulky substituents

rendered the pigments soluble in organic solvents and polymers and the pH sensitivity was preserved. On the other hand, alkylation of both lactam nitrogens is another simple way to greatly enhance the solubility of DPPs [52]. Evidently such modification renders the DPPs pH-insensitive. Mono-*N*-alkylation of the commercially available ‘Pigment Orange 73’ (scheme 1) with a *tert*-butylbenzyl-group preserves pH sensitivity and dramatically improves the solubility of the dye in such common solvents as toluene, tetrahydrofuran (THF), dichloromethane, chloroform, etc. Thus, the dye becomes suitable for application in optical plastic carbon dioxide sensors.

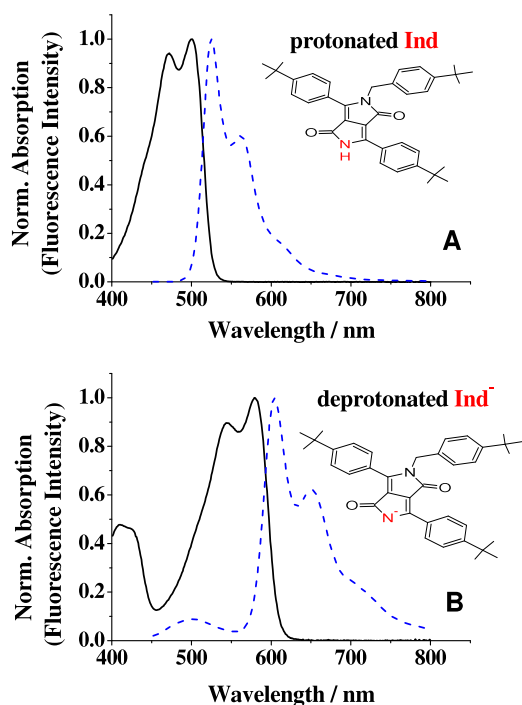
3.2. Photophysical properties

Absorption and emission spectra for DPtBu³ dissolved in THF are shown in figure 1. The protonated form of the dye absorbs in the blue and emits in the green part of the electromagnetic spectrum. Absorption and emission spectra for the deprotonated form are bathochromically shifted by ~ 70 nm compared to the protonated form. This is about 50 nm less than in case of previously reported DPP dye MoPh-DiSA (3,6-bis[4-bis(2-ethylhexyl)sulfonylamide-phenyl]-2,5-dihydropyrrolo[3,4-c]pyrrole-1,4-dione, table 1) [34]. The mono-alkylated dye shows spectral maxima at shorter wavelengths than not alkylated MoPh-DiSA. The molar absorption coefficients are typical for the DPP dyes (table 1). The fluorescence quantum yields are rather high and are comparable for both forms of DPtBu³ (table 1). On the contrary, the emission of the deprotonated form of MoPh-DiSA is much weaker than the emission of the protonated form.

DPtBu³ is highly soluble in organic solvents, but is not soluble in water. Therefore, determination of the pK_a in aqueous buffers is not possible. The pK_a value in a mixture of tetrahydrofuran and aqueous buffer (1:1 v/v) was estimated to be rather high (~ 12.7 ; supporting information, figure S1 available at stacks.iop.org/MAF/2/024001/mmedia). It should be noted that this is very rough estimation because of the high content of organic solvent and the alkali error of the pH electrode at high pH. The pK_a value for DPtBu³ is likely to be higher than that for the recently presented DPP dye (3,6-bis[4-(3')-disulfo-1,1'-biphenyl-4-yl]-2,5-dihydropyrrolo[3,4-c]pyrrole-1,4-dione dipotassium salt) [34] which showed a pK_a of ~ 11.8 since electron-donating *tert*-butyl groups of DPtBu³ are expected to elevate the dissociation constant.

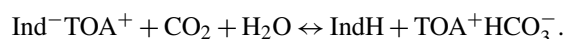
Table 1. Comparison of the photophysical properties of DPpTbu³ and the DPP dye MoPh-DiSA in tetrahydrofuran (THF) at 25 °C.

Dye	Protonated form			Deprotonated form		
	λ_{abs} ($\epsilon \times 10^{-3}$) (nm (M ⁻¹ cm ⁻¹))	λ_{em} (nm)	Φ	λ_{abs} ($\epsilon \times 10^{-3}$) (nm (M ⁻¹ cm ⁻¹))	λ_{em} (nm)	Φ
DPpTbu ³	472(25.2); 501(26.8)	524	0.86	572(17.6)	605	0.66
MoPh-DiSA	491(29.8); 528(36.9)	543;583	1	655(23.0)	708	0.11

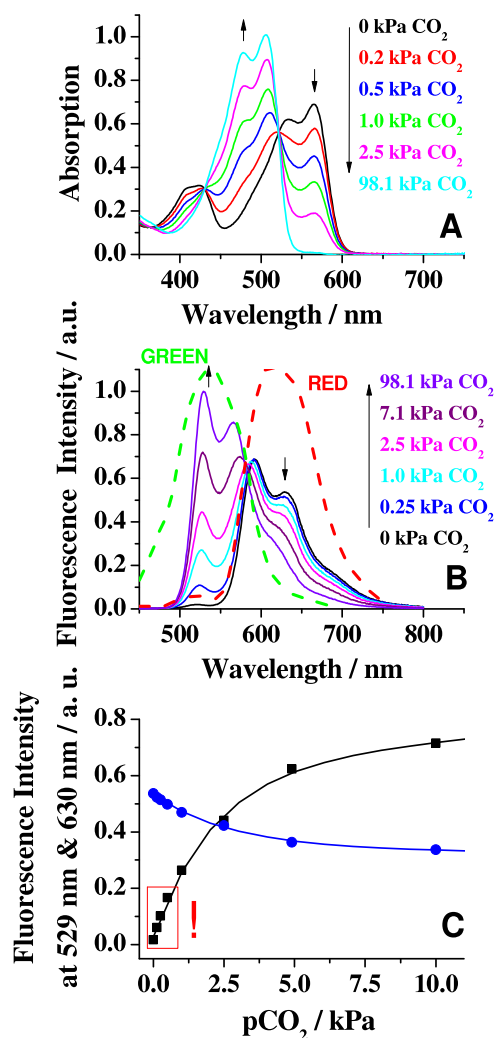
**Figure 1.** Absorption (solid lines) and emission (λ_{exc} 430 nm, dashed lines) spectra of the protonated form (A) and the deprotonated form (B) of DPpTbu³ in THF.

3.3. Carbon dioxide sensors

DPpTbu³ and the base tetraoctylammonium hydroxide (TOAOH) were non-covalently entrapped in an ethyl cellulose (EC49) matrix to obtain plastic type carbon dioxide sensors. The response of the sensor can be described by the following equation:



It is essential that the carbon dioxide sensors are kept humid during the measurements to enable reversible and reliable response (supporting information, figure S3 available at stacks.iop.org/MAF/2/024001/mmedia). The sensors respond to increasing pCO₂ with a color change from pink in the absence of CO₂ to yellow in the presence of CO₂. This corresponds to the change in the absorption spectra of the sensing material (figure 2(A)). Isosbestic points (IP) at 430 and 522 nm are clearly visible which indicates that only two forms of the dye are present in the acid–base equilibrium. The sensor shows red fluorescence at low pCO₂ and green fluorescence at high pCO₂ (figure 2(B)). For emission measurements

**Figure 2.** Absorption (A) and emission (B) spectra (λ_{exc} 430 nm) of the CO₂ sensor based on DPpTbu³ in ethyl cellulose 49 and TOAOH as base including the spectral sensitivity for the green and the red detection channels of the RGB camera (green and red dotted lines, (B)). (C) the fluorescence intensity changes for the protonated form (at 529 nm, black curve) and the deprotonated form (at 630 nm, blue curve) with increasing pCO₂, the fit is performed according to the exponential growth/decay model, respectively; high relative signal changes at low pCO₂ values (red box and exclamation mark) are indicated.

commercially available intense LEDs emitting at wavelengths between 430 and 470 nm are suitable as excitation sources. As can be seen, the emission intensity of the deprotonated form decreases, whereas the intensity of the protonated form increases with increasing pCO₂ (figure 2(C)). Importantly,

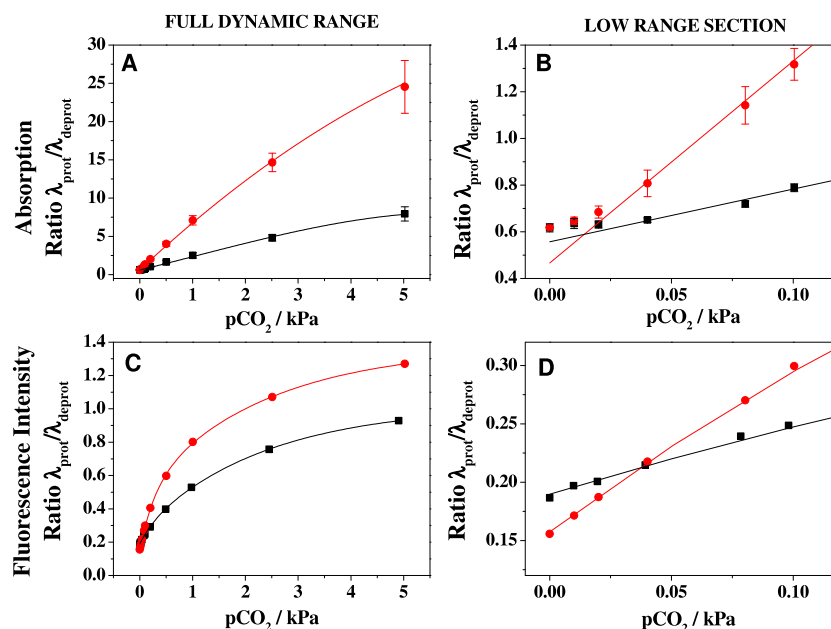


Figure 3. Absorption ((A), (B)) and emission ((C), (D)) calibration curves of carbon dioxide sensor based on DPpTbu³ for the full dynamic range from 0 to 4.9 kPa pCO₂ ((A), (C)) at 5 °C (red dots) and 25 °C (black squares) and for the respective low range sections ((B), (D)). A linear fit ((B), (D)), polynomial 2 fit (A) and exponential growth fit (C) were used.

virtually no fluorescence of the protonated form (λ_{\max} 529 nm) is detectable in the absence of carbon dioxide, so that the relative signal changes are very high at low pCO₂. Comparison of the absorption and emission spectra (figures 2(A) and (B)) indicates the effect of Förster resonance energy transfer (FRET) from the protonated form of the indicator to its deprotonated form. Indeed, the emission spectrum of the former and the absorption spectrum of the latter show almost perfect overlap (figure 1). The dye concentration dramatically affects the emission due to FRET (supporting information, figure S4 available at stacks.iop.org/MAF/2/024001/mmedia). For example, in case of high dye concentration (1.5% w/w) the emission spectrum is dominated by the deprotonated form at pCO₂ below 5 kPa. Hence, the dynamic range of the sensing materials relying on fluorescence intensity read-out can be tuned by adjusting the concentration of the indicator dye. Highly sensitive fluorescent sensors are obtained only for relatively low dye concentrations.

Compared to the solution the spectral properties of the indicator are mostly preserved (figures 1 and 2). The fluorescence quantum yields are high ($\Phi \approx 1.0$ and 0.63) for the protonated form and the deprotonated form, respectively. Carbon dioxide sensors based on DPpTbu³ are highly sensitive to pCO₂ at 25 °C (red box and exclamation mark in figure 2(C)). Due to better solubility of CO₂ at lower temperatures, the sensitivity is even higher at 5 °C (figure 3). It should be mentioned that rather strong temperature dependence is common for the ‘plastic type’ carbon dioxide sensors [8], but development of the materials with lower temperature cross-talk was beyond the scope of this study. Low levels of pCO₂ need to be measured in a completely decarbonated system—from gas lines, gas mixing device and humidifier to the flow-through cell—which is

difficult to achieve in practice. Particularly, precise calibration at the atmospheric level of 0.04 kPa pCO₂ and lower is challenging. The exchange of PET foil to gas-impermeable glass support improved the linearity at low pCO₂, but did not solve the contamination problem entirely. This is well observable in the absorption measurements where such contamination results in larger deviation than during fluorescence measurements influenced by FRET (figures 3(B) and (D), respectively). Determination of the limit of detection (LOD) was therefore not possible. Nevertheless, it can be concluded that the sensor shows excellent response at atmospheric levels (pCO₂ 0.04 kPa \approx 400 ppm in the gas phase \approx 13.6 $\mu\text{mol l}^{-1}$ in water at 298.15 K) of carbon dioxide and therefore is highly promising for e.g. oceanographic applications.

3.4. Photostability

The sulfonamide-based DPP indicators reported previously possessed adequate photostability for practical applications. Electron-withdrawing groups often improve the photostability of the fluorescent dyes and the electron-donating groups have an opposite effect [53]. Thus, photostability of DPpTbu³ bearing two electron-donating *tert*-butyl groups may be significantly lower than that for the sulfonamide-based indicators such as BiPh-DiSA [34]. However, photobleaching experiments carried out for the THF solutions of DPpTbu³ and BiPh-DiSA and an optical CO₂ sensor based on DPpTbu³ (using a high-power blue LED array, λ_{\max} = 458 nm, for the excitation of the protonated form of the dye; photon flux: \sim 4000 $\mu\text{mol s}^{-1} \text{m}^2$) revealed that the photostability of both dyes is very similar. Both dyes showed about 50% photodegradation in solution after 27 min of continuous

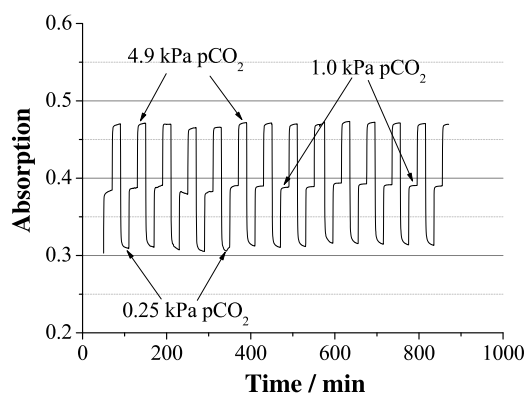


Figure 4. Absorption of the protonated form (505 nm) at alternating pCO₂ at 25 °C.

irradiation. Photostability of the optical sensor based on DPpTbu³ was very similar to that of the solution of the indicator (40 min for 50% photodegradation; supporting information, figure S2 available at stacks.iop.org/MAF/2/024001/mmedia). Thus, the new dye is suitable for practical applications. The light intensities necessary for the read-out of the sensors are typically much lower (10–100 fold) and only a pulse of short duration (20–50 ms) is required to obtain a measurement point. However, photobleaching can become more critical if very high light intensities are used such as in microscopy. In the absence of photobleaching the response of the sensor is fully reversible during prolonged measurements (figure 4).

3.5. RGB imaging

The emission of the protonated and deprotonated form of the sensing material shows excellent compatibility with the green and red channels, respectively, of a color camera (figure 2(B)). Importantly, both forms of the dye have comparable fluorescence quantum yields. Fluorescence imaging was performed using a consumer digital camera (Canon 5D). The change in the emission color can be easily distinguished with naked eye (figure 5). The intensity in the red channel does not change significantly ($\pm 10\%$) in the entire pCO₂ range. On the other hand the sensor shows dramatic increase of the signal in the green channel. Thus, referenced ratiometric imaging of pCO₂ with a simple set-up and using a single indicator dye becomes possible for the first time.

4. Conclusions

A new pH-sensitive indicator dye based on a diketo-pyrrolo-pyrrole chromophore is presented. A low cost starting pigment was chemically modified in one step via *N*-alkylation. The resulting dye is well soluble in organic solvents and polymers and is highly promising for preparation of carbon dioxide sensors. The features include high fluorescence quantum yields for the protonated and the deprotonated form of the dye and excellent compatibility of both emissions with the green and red channels of an RGB camera. These properties enable self-referenced ratiometric imaging of pCO₂ with a

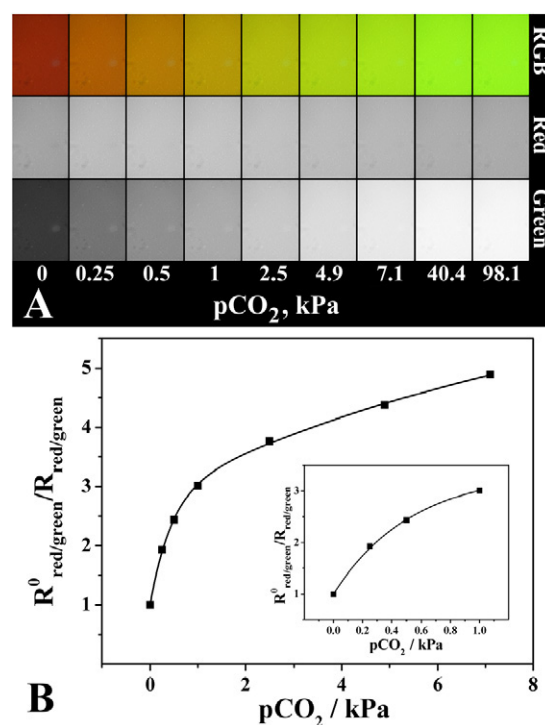


Figure 5. Photographic images of the planar optode based on DPpTbu³ under illumination with a 458 nm LED array acquired with a Canon 5D digital camera equipped with a long-pass ‘spring yellow’ filter (Lee filters) (A) and the respective calibration plot for the ratio of fluorescence intensities for the red and green channels (B). The inset shows the curve for low pCO₂ range.

single indicator. The optode shows excellent sensitivity at atmospheric levels of carbon dioxide. This makes the sensor a promising analytical tool for application in environmental monitoring, marine research and oceanography, for example for monitoring of ocean acidification.

Acknowledgments

This work was supported by 7th framework EU project ECO2, no 265847. We thank Robert Saf (Institute for Chemistry and Technology of Materials, Graz University of Technology, Austria) for mass spectrometry investigation.

References

- [1] Doney S C, Fabry V J, Feely R A and Kleypas J A 2009 Ocean acidification: the other CO₂ problem *Annu. Rev. Marine Science* **1** 169–92
- [2] Fabricius K E, Langdon C, Uthicke S, Humphrey C, Noonan S, De’ath G, Okazaki R, Muehllehner N, Glas M S and Lough J M 2011 Losers and winners in coral reefs acclimatized to elevated carbon dioxide concentrations *Nature Clim. Change* **1** 165–9
- [3] Fabry V J, Seibel B A, Feely R A and Orr J C 2008 Impacts of ocean acidification on marine fauna and ecosystem processes *ICES J. Mar. Sci.* **65** 414–32
- [4] Orr J C et al 2005 Anthropogenic ocean acidification over the twenty-first century and its impact on calcifying organisms *Nature* **437** 681–6

- [5] Rost B, Zondervan I and Wolf-Gladrow D 2008 Sensitivity of phytoplankton to future changes in ocean carbonate chemistry: current knowledge, contradictions and research directions *Mar. Ecol. Progr. Ser.* **373** 227–37
- [6] Riebesell U, Fabry V J, Hansson L and Gattuso J-P 2011 *Guide to Best Practices for Ocean Acidification Research and Data Reporting* (Luxembourg: Publications Office of the European Union)
- [7] Severinghaus J W and Bradley A F 1958 Electrodes for blood pO₂ and pCO₂ determination *J. Appl. Physiol.* **13** 515–20
- [8] Mills A, Lepre A and Wild L 1997 Breath-by-breath measurement of carbon dioxide using a plastic film optical sensor *Sensors Actuators B* **39** 419–25
- [9] Clegg M, Sullivan C and Eastin J 1978 Sensitive technique for rapid measurement of carbon-dioxide concentrations *Plant Physiol.* **62** 924–6
- [10] Arieli R, Ertracht O and Daskalovic Y 1999 Infrared CO₂ analyzer error: an effect of background gas (N-2 and O-2) *J. Appl. Physiol.* **86** 647–50
- [11] García-Fresnadillo D, Marazuela M D, Moreno-Bondi M C and Orellana G 1999 Luminescent Nafion membranes dyed with ruthenium(II) complexes as sensing materials for dissolved oxygen *Langmuir* **15** 6451–9
- [12] Liu Y, Tang Y, Barashkov N N, Irgibaeva I S, Lam J W Y, Hu R, Birimzhanova D, Yu Y and Tang B Z 2010 Fluorescent chemosensor for detection and quantitation of carbon dioxide gas *J. Am. Chem. Soc.* **132** 13951–3
- [13] Ali R, Lang T, Saleh S M, Meier R J and Wolfbeis O S 2011 Optical sensing scheme for carbon dioxide using a solvatochromic probe *Anal. Chem.* **83** 2846–51
- [14] Pandey S, Baker S N, Pandey S and Baker G A 2012 Optically responsive switchable ionic liquid for internally-referenced fluorescence monitoring and visual determination of carbon dioxide *Chem. Commun.* **48** 7043–5
- [15] Hong W, Chen Y, Feng X, Yan Y, Hu X, Zhao B, Zhang F, Zhang D, Xu Z and Lai Y 2013 Full-color CO₂ gas sensing by an inverse opal photonic hydrogel *Chem. Commun.* **49** 8229–31
- [16] Mills A, Chang Q and McMurray N 1992 Equilibrium studies on colorimetric plastic film sensors for carbon-dioxide *Anal. Chem.* **64** 1383–9
- [17] Mills A and Monaf L 1996 Thin plastic film colorimetric sensors for carbon dioxide: effect of plasticizer on response *Analyst* **121** 535–40
- [18] Mayr T, Klimant I, Wolfbeis O S and Werner T 2002 Dual lifetime referenced optical sensor membrane for the determination of copper(II) ions *Anal. Chim. Acta* **462** 1–10
- [19] Huber C, Klimant I, Krause C and Wolfbeis O S 2001 Dual lifetime referencing as applied to a chloride optical sensor *Anal. Chem.* **73** 2097–103
- [20] Liebsch G, Klimant I, Krause C and Wolfbeis O S 2001 Fluorescent imaging of pH with optical sensors using time domain dual lifetime referencing *Anal. Chem.* **73** 4354–63
- [21] Xu Z, Rollins A, Alcalá R and Marchant R E 1998 A novel fiber-optic pH sensor incorporating carboxy SNAFL-2 and fluorescent wavelength-ratiometric detection *J. Biomed. Mater. Res.* **39** 9–15
- [22] Hunter R C and Beveridge T J 2005 Application of a pH-sensitive fluorophore (C-SNARF-4) for pH microenvironment analysis in *Pseudomonas aeruginosa* biofilms *Appl. Environ. Microbiol.* **71** 2501–10
- [23] Spitzer K W, Skolnick R L, Peercy B E, Keener J P and Vaughan-Jones R D 2002 Facilitation of intracellular H⁺ ion mobility by CO₂/HCO₃⁻ in rabbit ventricular myocytes is regulated by carbonic anhydrase *J. Physiol.* **541** 159–67
- [24] Ramshesh V K and Lemasters J J 2012 Imaging of mitochondrial pH using SNARF-1 *Mitochondrial Bioenergetics: Methods and Protocols (Methods in Molecular Biology)* vol 810 ed C M Palmeira, A J Moreno and Herausgeber pp 243–8
- [25] Liebsch G, Klimant I, Frank B, Holst G and Wolfbeis O S 2000 Luminescence lifetime imaging of oxygen, pH, and carbon dioxide distribution using optical sensors *Appl. Spectrosc.* **54** 548–59
- [26] Wang X, Meier R J and Wolfbeis O S 2013 Fluorescent pH-sensitive nanoparticles in an Agarose matrix for imaging of bacterial growth and metabolism *Angew. Chem. Int. Edn* **52** 406–9
- [27] Schreml S, Meier R J, Wolfbeis O S, Landthaler M, Szeimies R-M and Babilas P 2011 2D luminescence imaging of pH *in vivo* *Proc. Natl Acad. Sci. USA* **108** 2432–7
- [28] Peng H, Stolwijk J A, Sun L-N, Wegener J and Wolfbeis O S 2010 A nanogel for ratiometric fluorescent sensing of intracellular pH values *Angew. Chem. Int. Edn* **49** 4246–9
- [29] Aigner D, Ungerboeck B, Mayr T, Saf R, Klimant I and Borisov S M 2013 Fluorescent materials for pH sensing and imaging based on novel 1,4-diketopyrrolo-[3,4-c]pyrrole dyes *J. Mater. Chem. C* **1** 5685–93
- [30] Wang X, Meier R J, Link M and Wolfbeis O S 2010 Photographing oxygen distribution *Angew. Chem. Int. Edn* **49** 4907–9
- [31] Kondrashina A, Dmitriev R, Borisov S, Klimant I, O'Brien I, Nolan Y M, Zhdanov A and Papkovsky D 2013 A phosphorescent nanoparticle based probe for sensing and imaging of (intra)cellular oxygen in multiple detection modalities *Adv. Funct. Mater.* **22** 4931–9
- [32] Larsen M, Borisov S M, Grunwald B, Klimant I and Glud R N 2011 A simple and inexpensive high resolution color ratiometric planar optode imaging approach: application to oxygen and pH sensing *Limnol. Oceanogr. Methods* **9** 348–60
- [33] Staal M, Borisov S M, Rickelt L F, Klimant I and Kuhl M 2011 Ultrabright planar optodes for luminescence life-time based microscopic imaging of O-2 dynamics in biofilms *J. Microbiol. Methods* **85** 67–74
- [34] Schutting S, Borisov S M and Klimant I 2013 Diketo-pyrrolo-pyrrole dyes as new colorimetric and fluorescent pH indicators for optical carbon dioxide sensors *Anal. Chem.* **85** 3271–9
- [35] Zollinger H 2003 *Color Chemistry: Syntheses, Properties, and Applications of Organic Dyes and Pigments* (New York: Wiley)
- [36] Luňák S Jr, Vala M, Vyňuchal J, Ouzzane I, Horáková P, Možíšková P, Eliáš Z and Weiter M 2011 Absorption and fluorescence of soluble polar diketo-pyrrolo-pyrroles *Dyes Pigments* **91** 269–78
- [37] Wong W W H, Subbiah J, Puniredd S R, Purushothaman B, Pisula W, Kirby N, Müllen K, Jones D J and Holmes A B 2012 Liquid crystalline hexa-peri-hexabenzocoronene-diketopyrrolopyrrole organic dyes for photovoltaic applications *J. Mater. Chem.* **22** 21131–7
- [38] Qu S, Wu W, Hua J, Kong C, Long Y and Tian H 2010 New diketopyrrolopyrrole (DPP) dyes for efficient dye-sensitized solar cells *J. Phys. Chem. C* **114** 1343–9

- [39] Qu S and Tian H 2012 Diketopyrrolopyrrole (DPP)-based materials for organic photovoltaics *Chem. Commun.* **48** 3039–51
- [40] Langhals H, Potrawa T, Nöth H and Linti G 1989 The influence of packing effects on the solid-state fluorescence of diketopyrrolopyrroles *Angew. Chem. Int. Edn Engl.* **28** 478–80
- [41] Langhals H, Grundei T, Potrawa T and Polborn K 1996 Highly photostable organic fluorescent pigments—a simple synthesis of *N*-arylprrrolopyrrolediones (DPP) *Liebigs Ann.* **1996** 679–82
- [42] Lorenz I-P, Limmert M, Mayer P, Piotrowski H, Langhals H, Poppe M and Polborn K 2002 DPP dyes as ligands in transition-metal complexes *Chem.—Eur. J.* **8** 4047–55
- [43] Langhals H, Limmert M, Lorenz I-P, Mayer P, Piotrowski H and Polborn K 2000 Chromophores encapsulated in gold complexes: DPP dyes with novel properties *Eur. J. Inorg. Chem.* **2000** 2345–9
- [44] Qu Y, Hua J and Tian H 2010 Colorimetric and ratiometric red fluorescent chemosensor for fluoride ion based on diketopyrrolopyrrole *Org. Lett.* **12** 3320–3
- [45] Jeong Y-H, Lee C-H and Jang W-D 2012 A diketopyrrolopyrrole-based colorimetric and fluorescent probe for cyanide detection *Chem.—Asian J.* **7** 1562–6
- [46] Yamagata T, Kuwabara J and Kanbara T 2010 Synthesis of highly fluorescent diketopyrrolopyrrole derivative and two-step response of fluorescence to acid *Tetrahedron Lett.* **51** 1596–9
- [47] Lebourgeois V, Bégué A, Labbé S, Mallavan B, Prévot L and Roux B 2008 Can commercial digital cameras be used as multispectral sensors? A crop monitoring test *Sensors* **8** 7300–22
- [48] Demas J and Crosby G 1971 Measurement of photoluminescence quantum yields—review *J. Phys. Chem.* **75** 991
- [49] Seybold G and Wagenblast G 1989 New perylene and violanthrone dyestuffs for fluorescent collectors *Dyes Pigment* **11** 303–17
- [50] Ford W 1987 Photochemistry of 3,4,9,10–perylene-tetracarboxylic dianhydride dyes—visible absorption and fluorescence of the Di(glycyl)imide derivative monomer and dimer in basic aqueous-solutions *J. Photochem.* **37** 189–204
- [51] Vala M, Vynuchal J, Toman P, Weiter M and Lunak S 2010 Novel, soluble diphenyl-diketo-pyrrolopyrroles: experimental and theoretical study *Dyes Pigment* **84** 176–82
- [52] Vala M, Weiter M, Vynuchal J, Toman P and Lunak S 2008 Comparative studies of diphenyl-diketo-pyrrolopyrrole derivatives for electroluminescence applications *J. Fluoresc.* **18** 1181–6
- [53] Weidgans B M, Krause C, Klimant I and Wolfbeis O S 2004 Fluorescent pH sensors with negligible sensitivity to ionic strength *Analyst* **129** 645–50